Non-First-Break Solution for Shallow Velocity Anomaly Problem*

Emil Blias[1]

Search and Discovery Article #41602 (2015)
Posted March 20, 2015

*Adapted from extended abstract prepared in conjunction with a presentation given at CSPG/CSEG 2006 GeoConvention, Calgary, AB, Canada, May 15-18, 2006,

[1]SeisVS, Calgary, Alberta, Canada (emilb@shaw.ca)

Abstract

A method of compensation for the presence of discrete shallow velocity anomalies (SVAs) has been developed. When the first breaks approach fails for any reason (first breaks are hard to pick, there is a shallow low velocity layer, permafrost etc) the only seismic information available is deep reflections. Shallow velocity anomalies cause large lateral variations in stacking velocities increasing with depth. Dix's formula gives us interval velocities in 1-D media. In many cases, the 1D assumption does not work, especially when we have local velocity anomalies in the overburden. Not only do they reduce post-stack image quality, but also create large differences in stacking velocity behaviour for deep seismic reflectors with small dips. A non-fist-breaks technology provides us tools to determine shallow velocity structures and remove their influence on stacking velocities and imaging. This technology includes four main steps: (i) High-density automatic non-hyperbolic NMO picking, (ii) Analytical NMO inversion to estimate shallow velocity structure, (iii) Non-linear horizon based traveltime tomography to improve depth velocity model and (iv) time-dependent velocity replacement corrections for prestack data. Model and real data examples show the practical feasibility and robustness of the proposed approach if there are deep consistent reflections.

Possibility of Simple Shallow Velocity Description

Conventional approach to deal with SVAs utilizes first breaks to determine shallow velocity structures (Hampson and Russell, 1984, Yilmaz, 1987, Taner et al., 1998, Cox, 1999). The presented approach deals only with deep reflections, which are supposed to be quite consistent. It is based on some theoretical results relating to NMO Dix's type inversion for a medium with curvilinear boundaries and laterally changing velocities. To describe SVAs, we use one layer with a laterally changing interval velocity. Because we do not use first breaks, a question arises: can we use this simple description of shallow velocity structures while they may be much more complicated, including several inhomogeneous curvilinear layers? It can be proved theoretically that for a subsurface with modest structures we can use a simple one-layer shallow velocity model to describe it such that vertical times in this layer will be very close to those of the initial complicated model.

The proof is based on an approximate formula derived by Blias (2005a, 2005b) for the NMO velocity:

$$\frac{1}{V_{NMO}^2(x)} = \frac{1}{V_{RMS}^2(x)}\left\{1 + V_{AVE}H\left(1 - \frac{F(x)}{H}\right)^2 \sum_{m=1}^{n}\left[\left(\frac{1}{V_m} - \frac{1}{V_{m+1}}\right)F_m''(x) + h_m s_m''(x)\right]\right\} \qquad (1)$$

Here V_m is an interval velocity in the m^{th} layer, $s_m=1/v_m$ is the slowness in the same layer, h_m is the thickness, V_{AVEm} is an average velocity between the anomaly depth F_m and the reflector depth H; F(x) is an average of anomaly depths and V_{AVE} is an average velocity between F and H. Let us consider the shallow portion of the subsurface with a horizontal bottom boundary. We assume that an adequate velocity model for this layer should be described with several curvilinear inhomogeneous layers. Let n be the number of the layers in this shallow part, $F_k(x)$ be the boundary and $v_k(x)$ be the interval velocity in this layer. Then the vertical time in this shallow structure is given by the formula:

$$t_{Vert}(x) = \sum_{k=1}^{n-1}\left(\frac{1}{V_k} - \frac{1}{V_{k+1}}\right)F_k(x) + \frac{H}{V_n} + \sum_{k=1}^{n} h_k s_k(x) \qquad (2)$$

We substitute all these n layers with one with the same bottom boundary H and with the slowness s(x). For static correction purpose, we want the zero-offset times to be the same. Since the zero offset time in the substitute layer is Hs(x) then from (2) it follows that slowness s(x) in this new layer satisfies the equation:

$$\sum_{k=1}^{n-1}\left(\frac{1}{V_k} - \frac{1}{V_{k+1}}\right)F_k(x) + \frac{H}{V_n} + \sum_{k=1}^{n} h_k s_k(x) = Hs(x)$$

After differentiating this equation two times, we come to the connection between the second-order derivatives of the two forms:

$$\sum_{k=1}^{n-1}\left(\frac{1}{V_k} - \frac{1}{V_{k+1}}\right)F_k''(x) + \sum_{k=1}^{n} h_k s_k''(x) = Hs''(x) \qquad (3)$$

For the model with a horizontal shallow layer with slowness, s(x) formula (1) becomes:

$$\frac{1}{V_{NMO}^2(x)} = \frac{1}{V_{RMS}^2(x)}\left[1 + s''(x)H\left(1 - \frac{F}{H}\right)^2 HV_{AVE}\right] \qquad (4)$$

Comparing formulas (1) and (4) and taking into account formula (3), we see that both SVA descriptions give close NMO velocities. This can be confirmed by modeling. The fact that, for deep reflections, we can replace complex shallow velocity structure with one shallow layer with

laterally changing interval velocity plays an important role in the non-first-break approach for determination of SVAs and removing their influence.

Main Steps of Non-First-Breaks Technology

Let us consider the main steps of the technology.

1. High-density NMO picking. Because SVAs cause strong lateral fluctuations of deep stacking velocities (Blias 1981, 1988, 2005a, 2005b), we need high-density velocity picking. Here the final goal is to pick NMO functions regardless of their shape. NMO information will be used to build depth velocity model including SVAs. We solve this problem with two steps. First we run constrained hyperbolic velocity analysis based on coherence semblances. The distinguishing feature of this step is that one has to manually pick velocities at one CDP gather. After that the program will automatically (using some constraints) find stacking velocities for each CDP point within a moving time window where possible. Picked velocities are interpolated to each time sample and smoothed. After that, picked hyperbolic NMO functions are applied to CDP gathers and NMO gathers are stacked. Then, one picks horizons and applies horizon-based residual non-hyperbolic moveout. Finally, we have NMO curves for several (picked) horizons that will be used in non-linear traveltime inversion.

2. Analytical NMO inversion to create a zero approximation for depth velocity model. For this, we use stacking velocities after the first velocity hyperbolic analysis. First, we determine a shallow velocity model using the method derived by Blias (2005c). After that, we use a generalization of the Dix formula a layered medium with lateral varying velocities (Blias, 2003). It allows us to determine the initial depth velocity model with curvilinear boundaries and laterally inhomogeneous layers.

3. Travel-time inversion and depth velocity model improvement. We use non-hyperbolic travel-times to build a depth velocity model, including shallow velocity structures. For this, we use an optimization approach (Blias and Khatchatrian, 2003). We describe interval velocities and boundaries as the sum of some reference (known) functions and linear combinations of basis functions with the coefficients to be found from minimizing an objective function. To find a minimum of the non-linear function F, we use the Newton method.

4. Velocity anomaly replacement (VAR). We use the depth velocity model to remove the influence of the SVA. For a given shallow velocity model it can be done by forward and reverse pre-stack wavefield extrapolation (Wapenaar and Berkhout, 1985). We use time-variable time shifts to remove the SVA effects, which is less expensive. For this, we run raytracing for the obtained depth velocity model and calculate prestack reflection time arrivals for all boundaries. Then we replace the shallow inhomogeneous layer with a homogeneous one and calculate time arrivals for this model. The difference between the first and the second set of times is applied to the CDP gathers. This procedure moves events on pre-stack data to the position where they would be if the shallow layer were homogeneous (Blias et al., 1985).

Model Data Test

Let us illustrate the above technique on model data. We test this approach on model data with modest deep structures. We will see that the suggested approach is stable and allows us to restore the depth velocity model when we have complicated SVA, caused by several curvilinear

boundaries and laterally inhomogeneous layers. Figure 1a shows a depth velocity model boundaries and interval velocities are displayed on Figure 1b. Red lines display interval velocities in the three shallow layers. From these figures, we see that the shallow part of the subsurface is complicated. The bottom of this shallow part is at 300m. Above this boundary, there are three curvilinear layers with laterally changing interval velocities. Average velocity in this layer is 1600 m/s. For this model synthetic CDP gathers have been calculated with maximum offset/ reflector depth = 1.5. Shot interval = receiver interval = 32 m. All five steps of the described technology have been run on this synthetic data. Figure 2a shows a velocity grid after automatic continuous velocity analysis. We see large lateral stacking velocity fluctuations increasing with depth.

An initial shallow velocity model was built, using method developed by Blias (2005b). We put h1 = 240m and average velocity in the first layer 1200m/s while h1 is 300m and average velocity in this layer is 1600 m/s. Here h1 is a thickness of the first layer. This means that we used wrong a priori parameters for the first layer to prove that it should not have much influence on the result of velocity anomaly replacement.

Figure 3 shows initial velocity in the first layer (red) and after optimization (brown). Except modest difference in shape, there is a constant shift because during traveltime inversion optimization we also changed the thickness of the first layer.

Because we took a wrong value for the bottom of the first layer with velocity anomalies (240 m instead of 300 m), the recovered velocity in this layer differs from the original average velocity. As was mentioned above, the vertical time should be found with reasonable accuracy. Figure 4 shows vertical times for the original model (blue) and for the model after traveltime inversion (brown). After we determined the interval velocity in the first layer, we use a generalization of Dix's formulas (Blias, 2003) to find interval velocities for the other layers. The results of these calculations give us an initial depth velocity model, which is needed for optimization-based traveltime inversion. To improve this model, traveltime optimization inversion was applied using non-hyperbolic traveltimes extracted after residual velocity analysis (Blias and Khatchatrian, 2003). Figure 5 shows boundaries of the initial model (brown) and after optimization traveltime inversion (blue). We see acceptable similarity between them. All structures were recovered correctly despite a wrong thickness of the first layer.

The model after traveltime inversion was used to calculate VAR corrections. These corrections were applied to the CDP gathers. They transform moveout curves to hyperbolic ones. Strictly speaking, new NMO curves are better approximated with hyperbolas than the original ones. VAR significantly removed non-hyperbolic distortions caused by shallow anomalies. VAR also significantly improved the velocity grid (Figure 2b) and structural imaging. Figure 6 shows poststack sections before (a) and after (b) VAR. We can see that after the VAR poststack data looks much more similar to the depth velocity model. From this, we conclude that, for the shallow part of the section, utilization of a laterally inhomogeneous layer instead of a complicated velocity model is acceptable. It allows us to restore SVA using deep reflections and to eliminate their influence on prestack gathers with sufficient accuracy.

Real Data Example

Let us demonstrate this approach on a real data example. This data has been obtained in an area where first breaks were very hard to pick. High-density non-hyperbolic constrained velocity analysis has been performed on CDP gathers. Figure 7a shows stacking velocities after automatic continuous constrained velocity analysis. We can see two anomalies in the interval 12-17 km, which caused large lateral variations

of stacking velocities from deep boundaries. The above inversion approach has been applied to stacking velocities. The horizon-based traveltime inversion was run using time arrivals as input data. Figure 8 shows depth velocity model obtained after traveltime inversion with two shallow velocity anomalies (red arrows in Figure 8b). Comparing Figure 8 a and b we see that after VAR stacking velocity show much less lateral variations, Figure 4b. Post-stack sections are shown in Figure 9. We see that VAR improved velocity grid and post-stack images.

Conclusions

To eliminate SVA effects, a non-first-break method has been presented. It uses a laterally inhomogeneous layer to describe the shallow part of the subsurface. To find the shallow velocity model, we use deep reflections picked after automatic high-density constrained velocity analysis. Stacking velocities are converted to a zero-approximation depth velocity model, which is improved by travel-time optimization inversion. Velocity replacement time-variant correction are calculated and applied to prestack gathers. This allows us to significantly remove the influence of SVAs on prestack data and to obtain more reliable images.

Acknowledgements

I would like to thank Valentina Khatchatrian who developed most of the software, Michael Burianyk (Shell Canada) for help with this paper and Samvel Khatchatrian for useful discussion.

References Cited

Blias E.A, 1981, Approximation of CDP traveltime for a layered medium with curved interfaces and variable layer velocities: Soviet Geology and Geophysics, N 11, p. 79-86.

Blias E., 1988, Time fields in 3D medium with curvilinear inhomogeneous layers: Mathematic problems in seismic: Novosibirsk, p. 98-127 (in Russian).

Blias, E., 2003, Dix's type formulae for a medium with laterally changing velocity: 73rd Intern., SEG Annual Meeting, Expanded Abstracts, p. 706-709.

Blias E., 2005a, Stacking and Interval Velocities in the presence of Overburden Velocity Anomalies: 67th EAGE Conference, Expanded abstracts, p. 175.

Blias, E., 2005b, Stacking velocities in the presence of shallow velocity anomalies: 75th Intern., SEG Meeting, Meeting, Expanded Abstracts, p. 2193-2196.

Blias, E., 2005c, Determination of shallow velocity anomalies using deep reflections: 75th Intern., SEG Meeting, Expanded Abstracts, p. 2585-2588.

Blias E., and V. Khatchatrian, 2003, Optimization approach to determine interval velocities in a medium with laterally inhomogeneous curvilinear layers: 73rd Intern., SEG Meeting, Expanded Abstracts, p. 670-763.

Blias E.A., A.N. Levit and V.N. Ferentsi, 1985, Method of taking into account shallow anomalies while processing CDP data: Directions and methodology in Oil and Gas Exploration, Nauka, (in Russian), p. 71-74.

Cox, M.J.G., 1999, Static corrections for seismic reflection surveys: Tulsa, OK, Society of Exploration Geophysicists, p. 1–531.

Hampson, D., and B. Russell, 1984, First break interpretation using generalized linear inversion: 54th Intern., SEG Meeting, Expanded Abstracts, p. 532–534.

Taner, M.T., D.E. Wagner, E. Baysal, and L. Lu, 1998, A unified method for 2-D and 3-D refraction statics: Geophysics, v. 63, p. 260–274.

Wapenaar, C.P.A., and A.J. Berkhout, 1985, Velocity determination in layered systems with arbitrarily curved interfaces by means of wave-field extrapolation of common-midpoint data: Geophysics, v. 50, p. 63-76.

Yilmaz, O., 1987, Seismic data processing: Tulsa, OK, Society of Exploration Geophysicists.

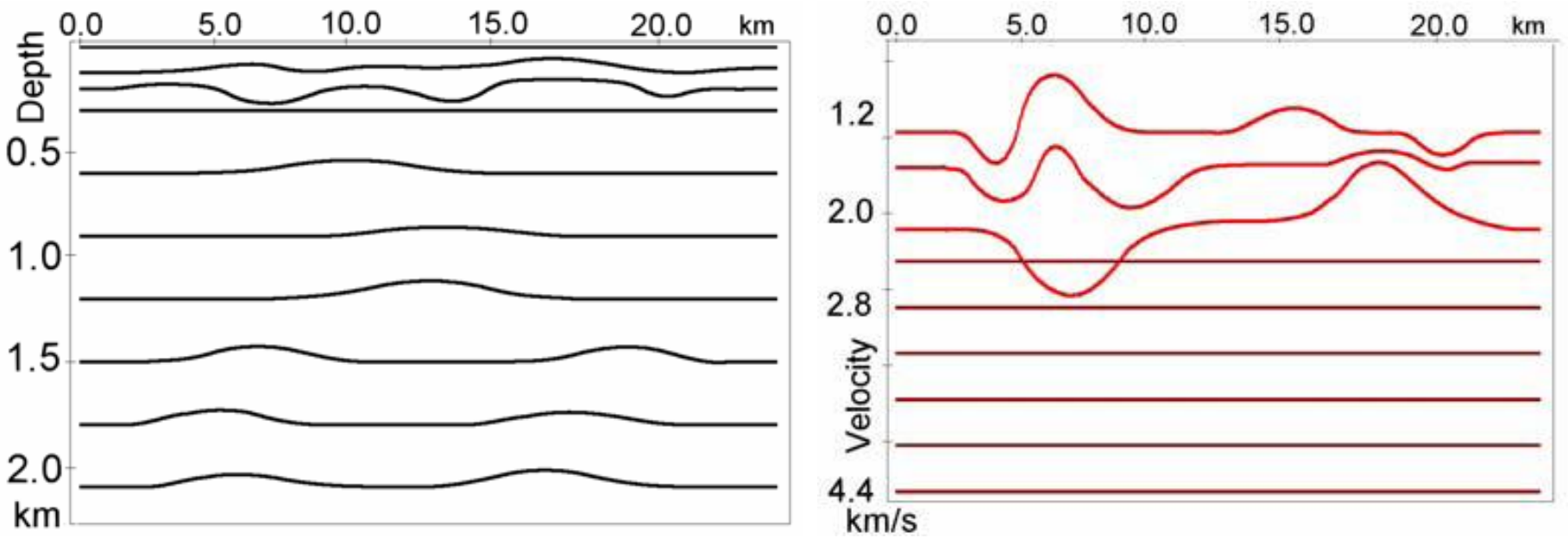

Figure 1. Depth velocity model boundaries (a) and interval velocities (b).

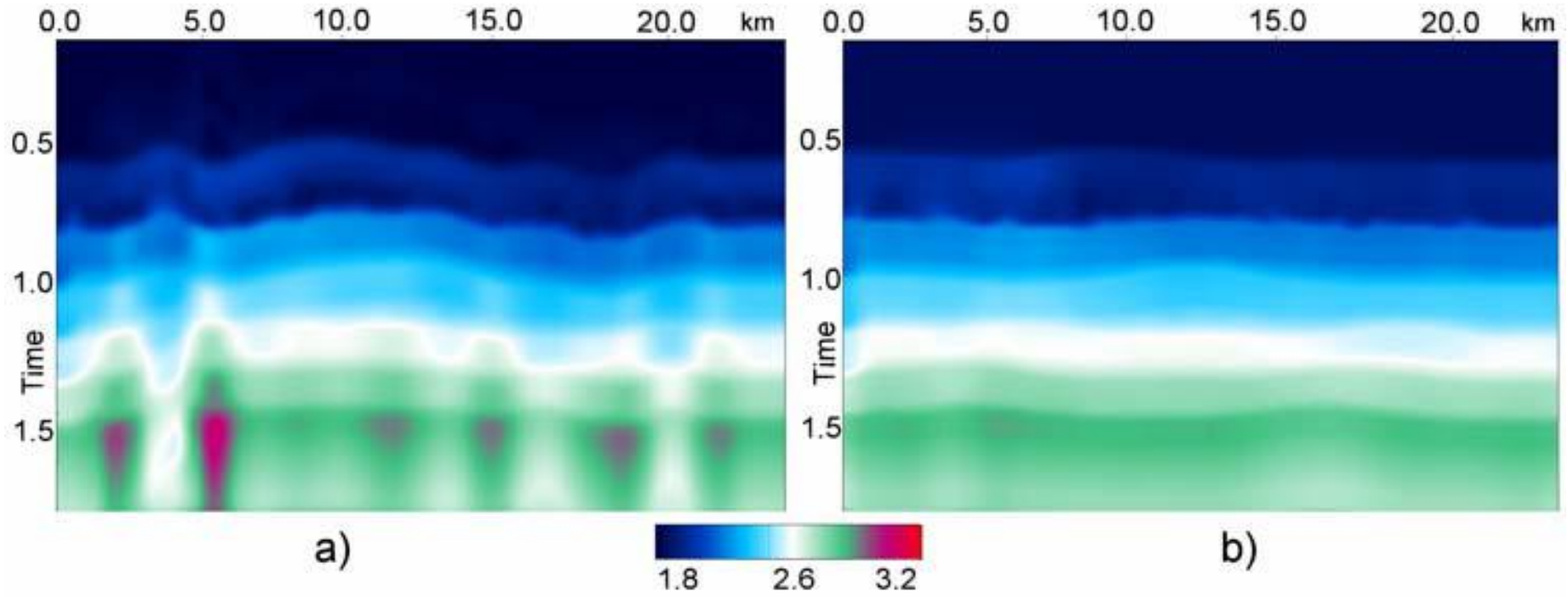

Figure 2. Velocity grid before (a) and after (b) VAR.

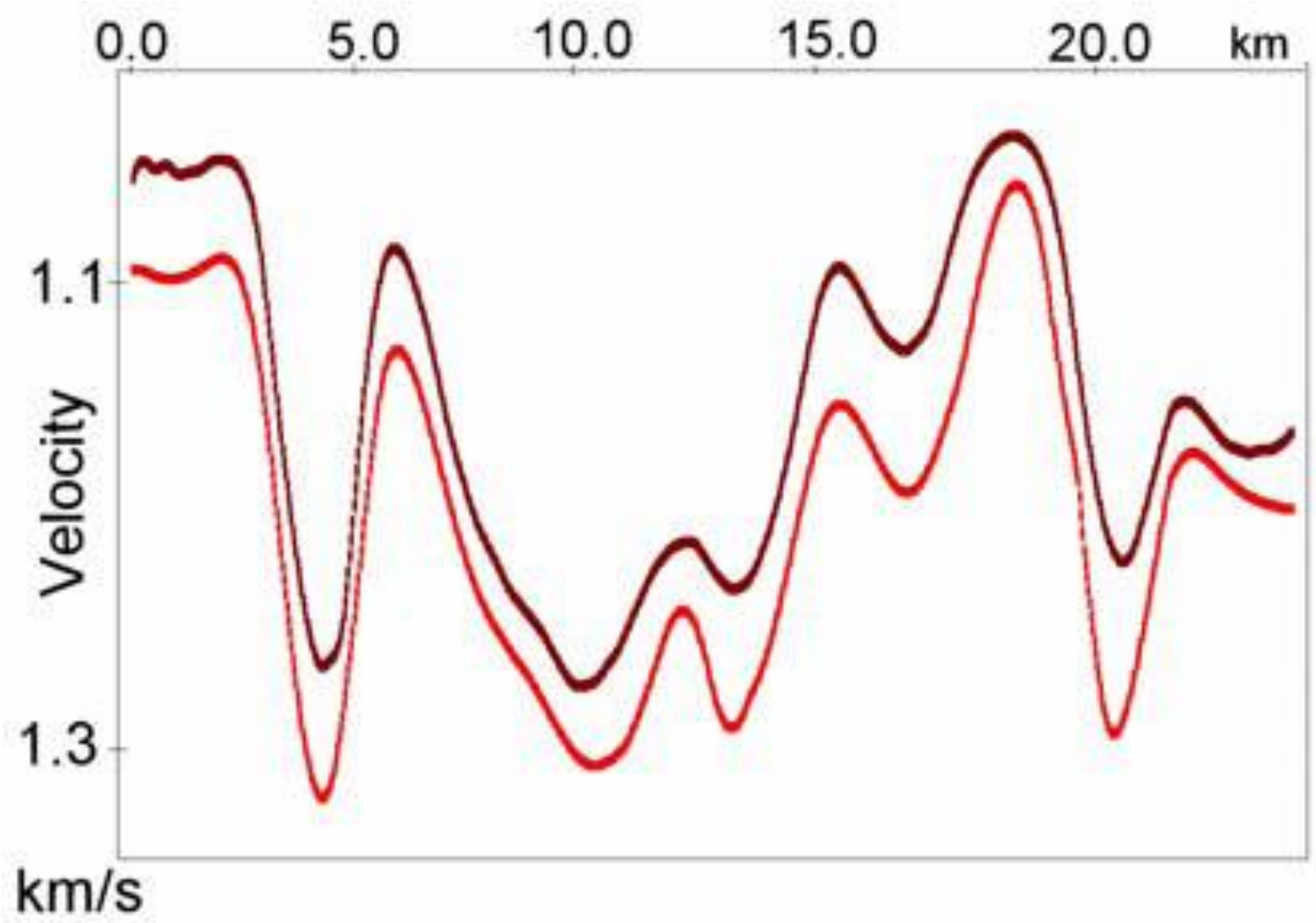

Figure 3. Velocity in the first layer after analytical inversion (red) and optimization (brown).

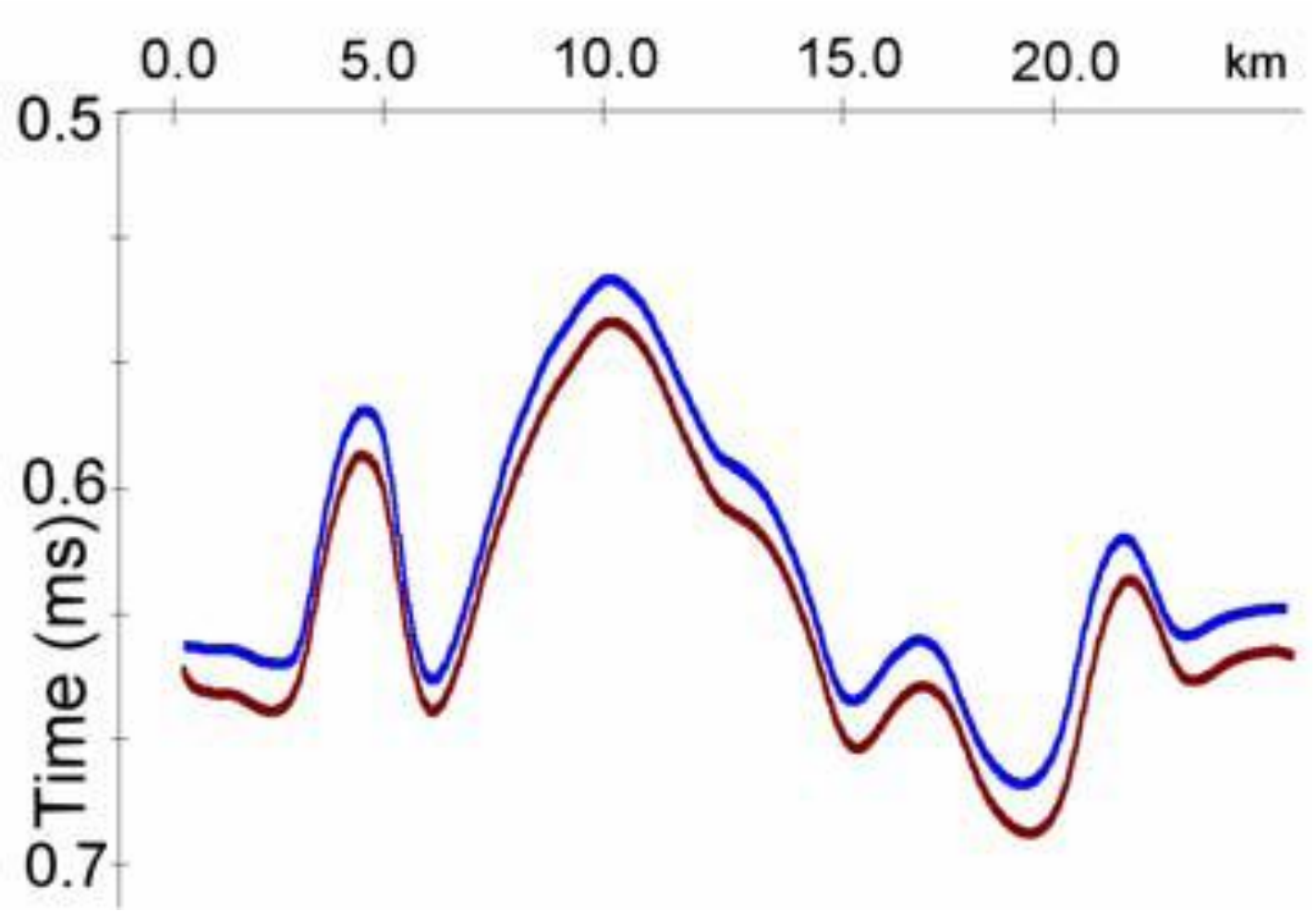

Figure 4. Vertical times in the first layer for initial model (blue) and recovered model (brown).

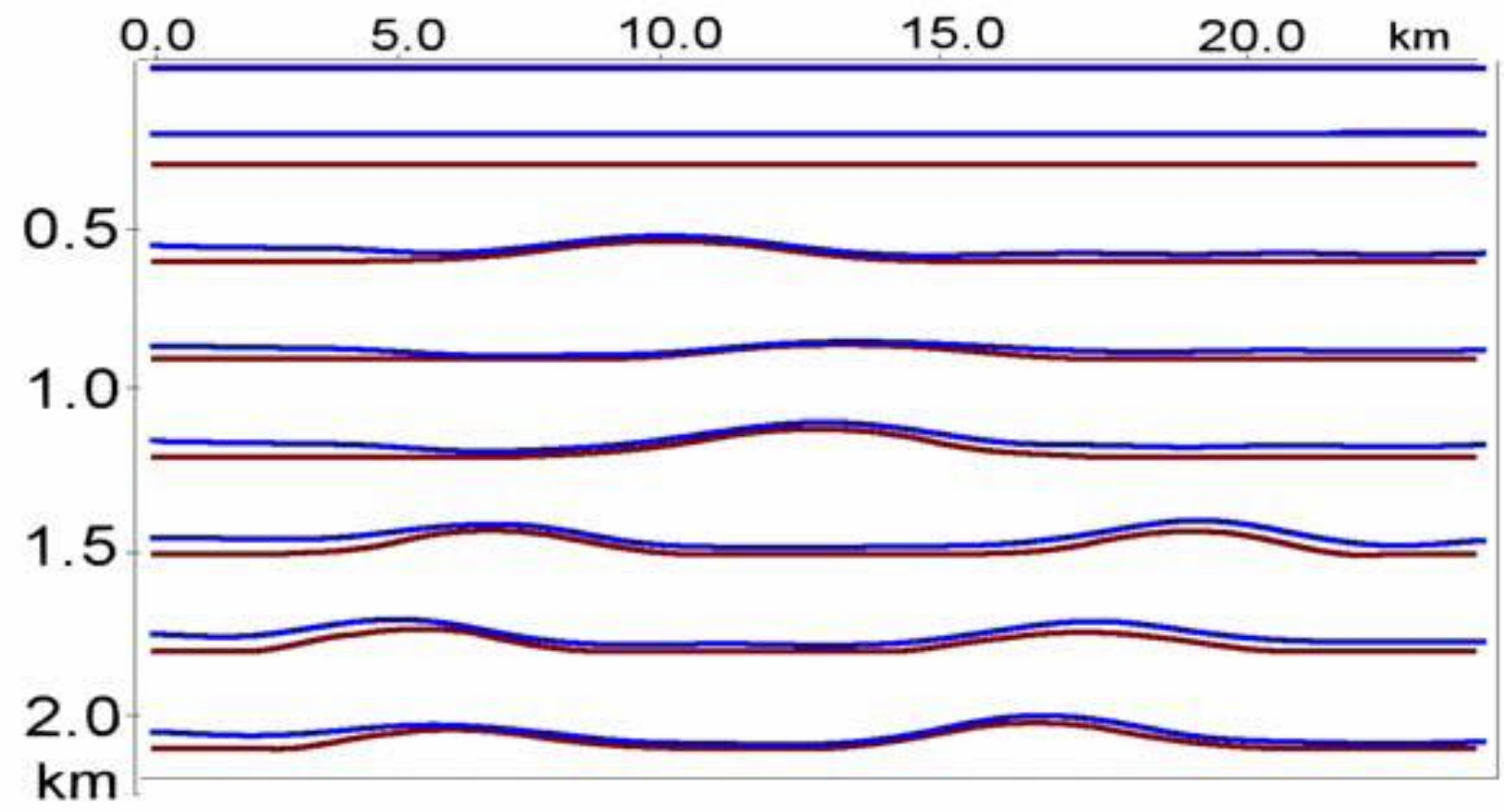

Figure 5. Boundaries of original model (brown) and after time-inversion (blue).

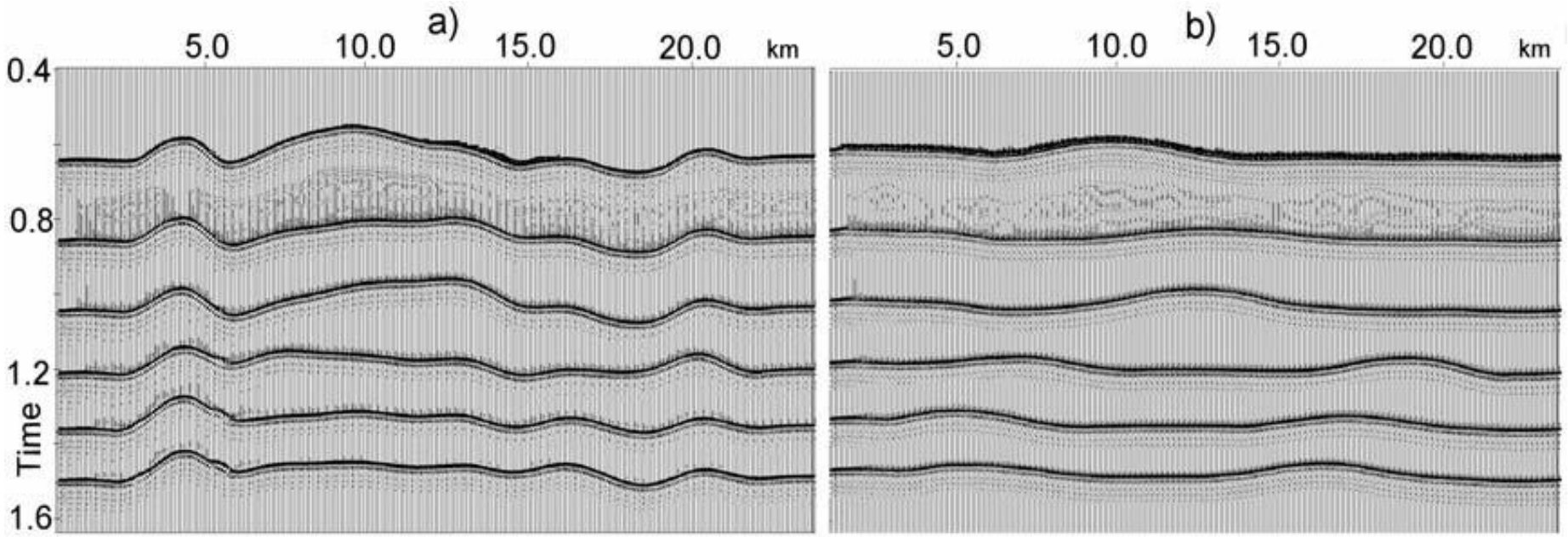

Figure 6. Poststack sections before (a) and after (b) VAR.

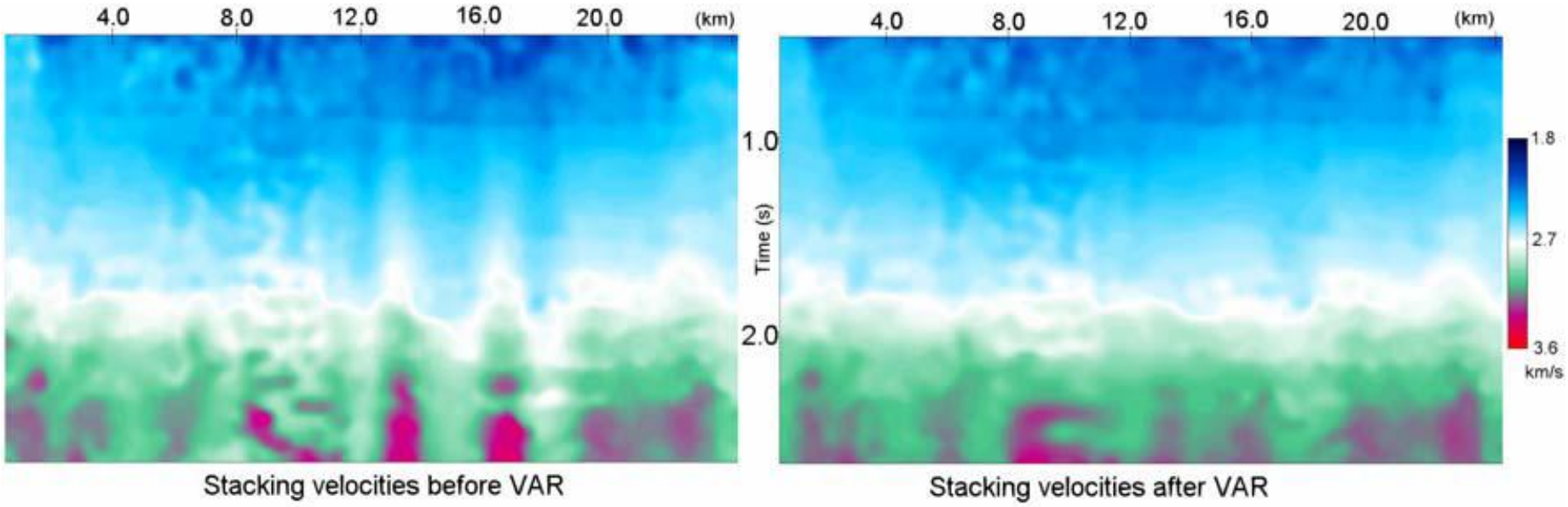

Figure 7. Stacking velocities before VAR (a) and after (b).

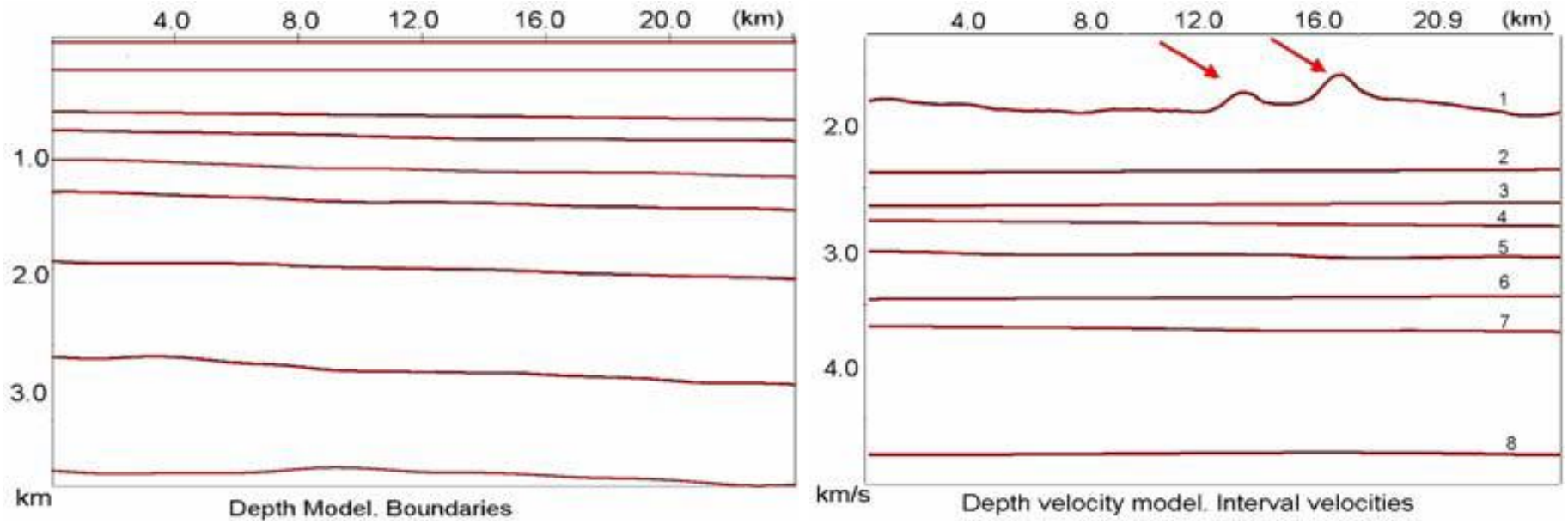

Figure 8. A) Boundaries figure; B) interval velocities.

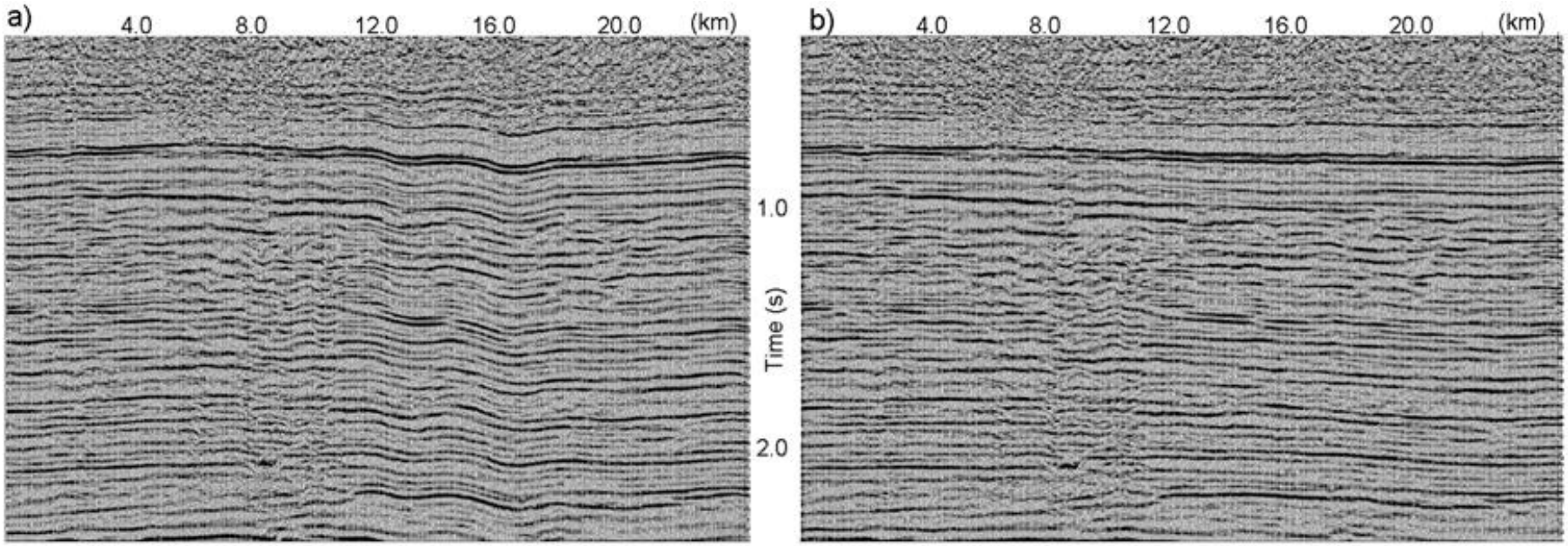

Figure 9. Poststack data: a – before VAR, b – after VAR.